Polymer Chemistry

PAPER

A new route to functional polymers: atom-economical synthesis of poly(pyrazolylnaphthalene)s by rhodium-catalyzed oxidative polycoupling of phenylpyrazole and internal diynes†

Meng Gao,[a] Jacky W. Y. Lam,[a] Yajing Liu,[a] Jie Li[a] and Ben Zhong Tang*[abc]

A new route for atom-economical synthesis of functional polymers was developed. Oxidative polycoupling of 3,5-dimethyl-1-phenylpyrazole with 4,4′-(α,ω-alkylenedioxy) bis(diphenylacetylene)s and 1,2-diphenyl-1,2-bis[4-(phenylethynyl)phenyl]ethene, respectively, were catalyzed by [Cp*RhCl₂]₂, 1,2,3,4-tetraphenylcyclopenta-1,3-diene and copper(II) acetate in dimethylformamide under stoichiometric imbalance conditions, affording soluble poly(pyrazolylnaphthalene)s in satisfactory yields (isolation yield up to 82%) with high molecular weights (M_w up to 35 700). All the polymers were thermally stable, losing little of their weight at high temperatures of 323–422 °C. They possessed good film-forming property and their thin solid films showed high refractive indices (RI = 1.747 − 1.593) in a wide wavelength region of 400–1000 nm. The polymer carrying tetraphenylethene units displayed a phenomenon of aggregation-induced emission and showed enhanced light emission in the aggregated state. The emission of its nanoaggregates could be quenched efficiently by picric acid in both solution and solid states, suggesting that it is a promising sensitive chemosensor for detecting explosives for real-world applications.
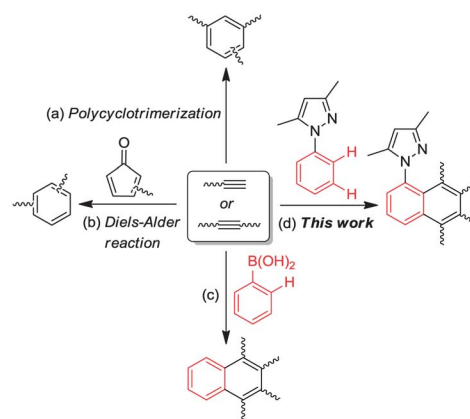
Introduction

Development of a new methodology for the synthesis of functional polymers is an important research area in macromolecular science. Olefins have been the main sources of monomers, whose addition polymerization yields polymers with electronically saturated backbones that are commonly used as commodity materials. Polymerization of acetylenic monomers can generate polymers with π-conjugated backbones that are expected to be electronically active. Indeed, polyacetylene was found to exhibit metallic conductivity upon doping by Shirakawa, MacDiarmid and Heeger in the 1970s.[1] This seminal discovery has triggered great efforts in utilizing alkynes as building blocks to construct functional polymers. As a result, a large number of π-conjugated polymers has been synthesized

from alkyne monomers.[2] Among various employed methods, the polycyclotrimerization or Diels–Alder reaction could afford polymers with stable benzene rings (Scheme 1),[3] and hence broad applications in organic light-emitting diodes,[4] photovoltaic cells[5] and sensors.[6]

Highly substituted naphthalene derivatives are well-known for their high thermal stability and unique electro- and

aDepartment of Chemistry, Institute for Advanced Study and Division of Biomedical Engineering, The Hong Kong University of Science & Technology (HKUST), Clear Water Bay, Kowloon, Hong Kong, China. E-mail: tangbenz@ust.hk

bGuangdong Innovative Research Team, SCUT-HKUST Joint Research Laboratory, State Key Laboratory of Luminescent Materials and Devices, South China University of Technology (SCUT), Guangzhou, 510640, China

cHKUST Shenzhen Research Institute, No. 9 Yuexing 1st RD, South Area, Hi-tech Park, Nanshan, Shenzhen, China 518057
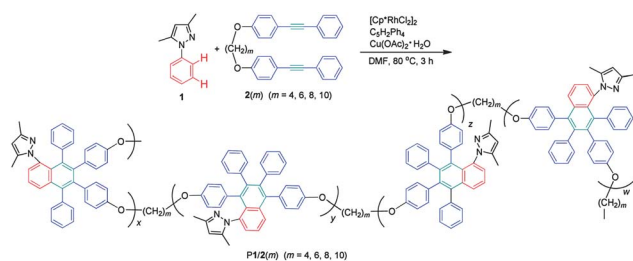
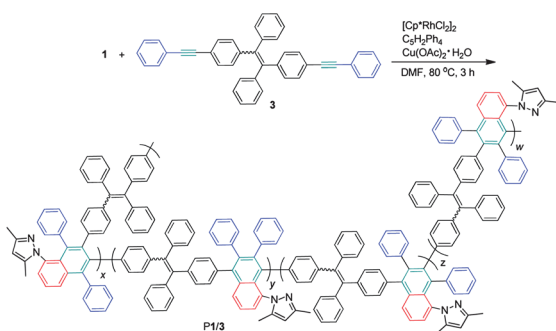**Scheme 1** Synthetic routes to polyarylenes by (a) alkyne polycyclotrimerization, (b) Diels–Alder reaction of an alkyne with cyclopenta-2,4-dienone and oxidative polycouplings of (c) phenylboronic acid with an internal alkyne and (d) phenylpyrazole with an internal alkyne.

Scheme 2 Rhodium-catalyzed oxidative polycoupling of phenylpyrazole **1** and internal diynes **2**(*m*).

photochemical properties, as well as their potential uses as organic semiconductors and luminescent materials.[7] Recently, we found that the rhodium-catalyzed oxidative polycoupling of arylboronic acids and internal diynes proceeded smoothly under stoichiometric imbalance-promoted conditions,[8] affording poly(naphthalene)s with moderate molecular weights in satisfactory yields (Scheme 1).[9] Thanks to their high aromatic content, the resulting polymers showed high thermal stability and were light refractive. Although the polymerization reactions generated boronic acids as byproducts, we would like to develop more "green" methodologies for atom-economical synthesis of functional polymers with high molecular weights for useful practical applications.

Satoh *et al.* recently reported a promising method for the preparation of pyrazolylnaphthalenes by rhodium-catalyzed oxidative coupling of phenylpyrazoles and internal alkynes.[10] This reaction is very interesting as the regioselective C–H bond activation or cleavage can be realized by the proximate effect of the pyrazole ring. Thus, this functional group will not be eliminated during the reaction. In other words, such reaction is efficient in atom economy and the products are of high purity. More importantly, the presence of an excess amount of phenylpyrazole in the reaction mixture can improve the reaction efficiency significantly, suggesting that it is promising to be developed into an atom-economical polymerization tool that operates under stoichiometric imbalance conditions. However, such a possibility has rarely been explored though a large number of low molecular weight pyrazolylnaphthalenes has been prepared *via* such a method. In this paper, we took such a challenge and showed that the poly(pyrazolylnaphthalene)s **P1/2**(*m*) and **P1/3** (Schemes 2 and 3) obtained under optimized

conditions exhibited novel thermal, photonic and photophysical properties.

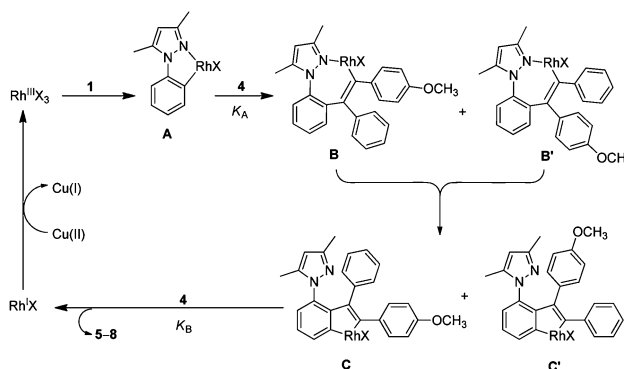## Results and discussion

Monomer synthesis

To develop the oxidative coupling of phenylpyrazole and internal alkyne into a versatile methodology for the construction of functional polymers, we synthesized 3,5-dimethyl-1-phenylpyrazole (**1**)[11] and 4,4′-(*α*,*ω*-alkylenedioxy) bis(diphenylacetylene) s **2**(*m*)[9] (Scheme 2) according to the literature methods. Considering that tetraphenylethene (TPE)[12] shows a phenomenon of aggregation induced emission (AIE), we also prepared 1,2-bis-[4-(2-phenylethynyl)phenyl]-1,2-diphenyl-ethene **3** (Scheme 3) by palladium-catalyzed cross-coupling of 1,2-bis(4-bromophenyl)-1,2-diphenylethene[13] and phenylacetylene, whose polymerization with **1** was expected to give a polymer with a fully conjugated structure. All the monomers were characterized by standard spectroscopic methods and gave satisfactory analysis data corresponding to their structures (see data given in the Experimental section).

Model reaction

Before studying the polymerization of **1** with **2**(*m*) or **3**, we first examined whether **1** could couple with an asymmetric internal alkyne **4** (Scheme 4).[9] The oxidative coupling reaction was catalyzed by [Cp*RhCl₂]₂ in the presence of Cu(OAc)₂·H₂O as an oxidant and 1,2,3,4-tetraphenylcyclopenta-1,3-diene (C₅H₂Ph₄)
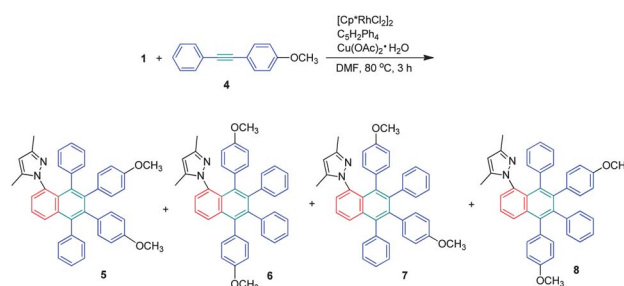
Scheme 4 Synthesis of pyrazolylnaphthalenes **5–8** by rhodium-catalyzed oxidative coupling of **1** and **4**.

Scheme 3 Polymerization of phenylpyrazole **1** and tetraphenylethene-containing internal diyne **3**.

Scheme 5 Mechanism for the formation of pyrazolylnaphthalenes **5–8**.

as a replacement ligand in dimethylformamide (DMF) at 80 °C under nitrogen, which furnished a mixture of pyrazolylnaphthalenes **5–8** in a total yield of 91% after purification. Since **5–8** possess similar physical properties, it is hard to separate them by column chromatography. They also resonate at very similar chemical shifts, thus preventing us to determine their molar ratios by ^{1}H NMR spectroscopy. However, their high resolution mass spectrum exhibited an M^+ peak at 586.2661, which was in good agreement with their calculated molar mass (586.2620) and hence confirmed their structures.

What is the mechanism for this reaction? It is believed that it involves first the coordination of **1** to $Rh^{III}X_3$ species by regioselective C–H bond cleavage to afford the intermediate **A** (Scheme 5). Then, insertion of **4** into the C–Rh bond of **A** formed intermediates **B** and **B′**, which underwent the second cyclorhodation at the 3′-position of the phenyl ring to give intermediates **C** and **C′**. The insertion of the second alkyne molecule into **C** and **C′** followed by reductive elimination afforded a mixture of **5–8**. The resulting Rh^IX species was oxidized by a copper(II) salt to regenerate $Rh^{III}X_3$. Since intermediates **C** and **C′** are more reactive than species **A**, the insertion of the second alkyne molecule is much faster than the first one ($K_A \ll K_B$). As a result, the presence of an excess amount of **1** in the reaction mixture will not affect but indeed improve the reaction efficiency. If a diyne monomer is used, alkyne groups will always exist at the chain ends, which suppresses undesirable intrachain cyclization that leads to the formation of polymers with low molecular weights.

Polymerization

Although **1** can be coupled with **4** efficiently under the conditions stated in Scheme 4, their suitability for the polymerization of **1** and **2**(*m*) or **3** remains uncertain. To search for optimum parameters, we first studied the effects of different oxidants and temperature on the oxidative polycoupling reaction using **1** and **2**(4) as monomers. In the presence of $Cu(OAc)_2 \cdot H_2O$, a polymer was obtained in a good yield of 82% with an M_w value of 26 300 at 80 °C for 3 h (Table 1, no. 1). Temperature exerted a strong influence on the polymerization: a polymer was isolated in a much lower yield of 26% at 60 °C (Table 1, no. 2). While silver salts such as AgOTs, $AgCF_3SO_3$ and $AgCF_3CO_2$ are good oxidants to oxidize Rh^IX to $Rh^{III}X_3$ (ref. 10) and for the polycoupling of phenylboronic acid and internal diyne,[9] we found that none of them was capable of initiating the polymerization (Table 1, no. 3–5).

The influence of monomer and catalyst concentrations on the polymerization was then investigated. When the concentrations of **1** and **2**(4) were increased progressively from 0.10 M and 0.50 M to 0.40 M and 0.20 M, respectively but keeping the monomer and catalyst feeding ratios unchanged, both the isolated yield and molecular weight of the polymer were enhanced accordingly (Table 2, no. 1–4). The polymerization of **1** and **2**(4) carried out at a molar ratio of 1 : 1 gave a poorer result (Table 2, no. 5). Thus, it seems that it is beneficial to perform the polymerization in an excess amount of **1** or under stoichiometric imbalance conditions.

Table 3 summarizes the polymerization of other monomer pairs under optimum conditions. All the polymerization

Table 1 Effects of oxidant and temperature on the polymerization of **1** and **2**(4)[a]

No.	Oxidant	Temp. (°C)	Yield (%)	$M_w{}^b$	$M_w/M_n{}^b$
1	$Cu(OAc)_2H_2O$	80	82	26 300	1.50
2	$Cu(OAc)_2H_2O$	60	26	24 600	1.89
3	AgOTs	80	0		
4	$AgCF_3SO_3$	80	0		
5	$AgCF_3CO_2$	80	0		

[a] Carried out in DMF under nitrogen for 3 h in the presence of $[Cp*RhCl_2]_2$, $C_5H_2Ph_4$ and different oxidants. [**1**] = 0.40 M, [**2**(4)] = 0.20 M, [Rh] = 8 mM. $[C_5H_2Ph_4]$ = 0.032 M and [oxidant] = 0.40 M. [b] Estimated by GPC in THF on the basis of a polystyrene calibration.

Table 2 Concentration effects on the polymerization of **1** and **2**(4)[a]

No.	[**1**] (M)	[**2**(4)] (M)	Yield (%)	$M_w{}^b$	$M_w/M_n{}^b$
1	0.10	0.05	61	19 400	2.19
2	0.15	0.075	68	22 600	1.85
3	0.20	0.10	76	25 100	1.70
4[c]	0.40	0.20	82	26 300	1.50
5	0.20	0.20	71	18 200	1.61

[a] Carried out in DMF at 80 °C under nitrogen for 3 h in the presence of $[Cp*RhCl_2]_2$, $C_5H_2Ph_4$ and $Cu(OAc)_2 \cdot H_2O$. Molar ratio of [**1**] : [**2**(4)] : [Rh] : $[C_5H_2Ph_4]$: [Cu] = 2.0 : 1.0 : 0.02 : 0.08 : 2.0. [b] Estimated by GPC in THF on the basis of a polystyrene calibration. [c] Data taken from Table 1, no. 1.

Table 3 Polymerization of **1** and **2**(*m*) or **3** under optimized conditions[a]

No.	Polymer	Yield (%)	$M_w{}^b$	$M_w/M_n{}^b$
1[c]	**P1/2(4)**	82	26 300	1.50
2	**P1/2(6)**	74	27 300	1.53
3	**P1/2(8)**	79	26 000	1.58
4	**P1/2(10)**	77	35 700	1.66
5	**P1/3**	66	17 900	1.71

[a] Conducted in DMF at 80 °C under nitrogen for 3 h in the presence of $[Cp*RhCl_2]_2$, $C_5H_2Ph_4$ and $Cu(OAc)_2 \cdot H_2O$. [**1**] = 0.40 M, [**2**(*m*)] = 0.20 M, [Rh] = 8 mM, $[C_5H_2Ph_4]$ = 32 mM and [Cu] = 0.40 M. [b] Estimated by GPC in THF on the basis of a polystyrene calibration. [c] Data taken from Table 1, no. 1.

reactions proceeded smoothly, giving their corresponding polymers **P1/2(*m*)** and **P1/3** in good yields with high molecular weights up to 35 700 and narrow distributions down to 1.5 (Table 3, no. 1–5). Even though they are constructed from aromatic rings, all the polymers show good solubility in common organic solvents, such as dichloromethane, chloroform, tetrahydrofuran (THF) and toluene, and can fabricate into tough, thin solid films by spin-coating or static-casting processes, presumably due to the irregular distribution of the repeating units of **5–8** along the polymer chains.

Structural characterization

All the polymers were characterized by standard spectroscopic methods and gave satisfactory analysis data corresponding to
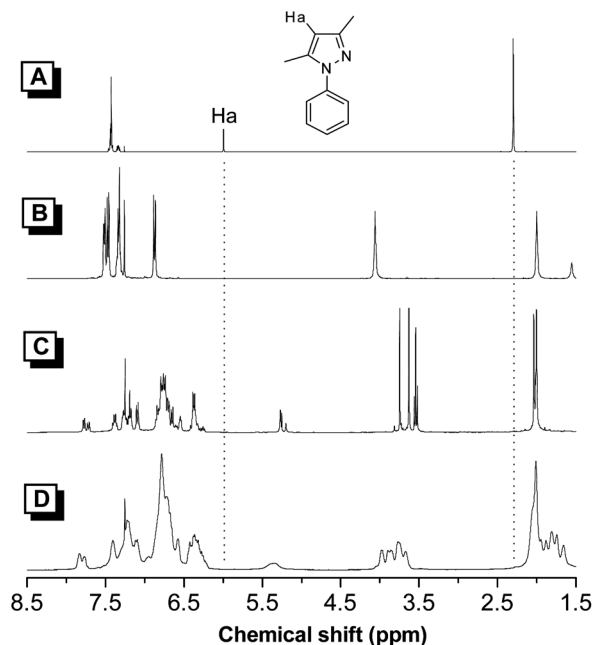
Fig. 1 ^{1}H NMR spectra of CDCl$_3$ solutions of (A) **1**, (B) **2**(4), (C) a mixture of **5–8** and (D) **P1/2**(4) (sample taken from Table 3, no. 1).

their structures. For example, the IR spectrum of **P1/2**(4) showed absorption peaks inherited from **1** and **2**(4) except that associated with C≡C stretching vibrations at 2218 cm^{-1} (Fig. S1 in the ESI†). Fig. 1 shows the ^{1}H NMR spectra of **P1/2**(4), **1**, **2**(4) and a mixture of model compounds **5–8**. The absorption peak at δ 5.99 in **1** was associated with the aromatic proton resonance of the pyrazole ring, which shifted upfield to δ 5.34 in the

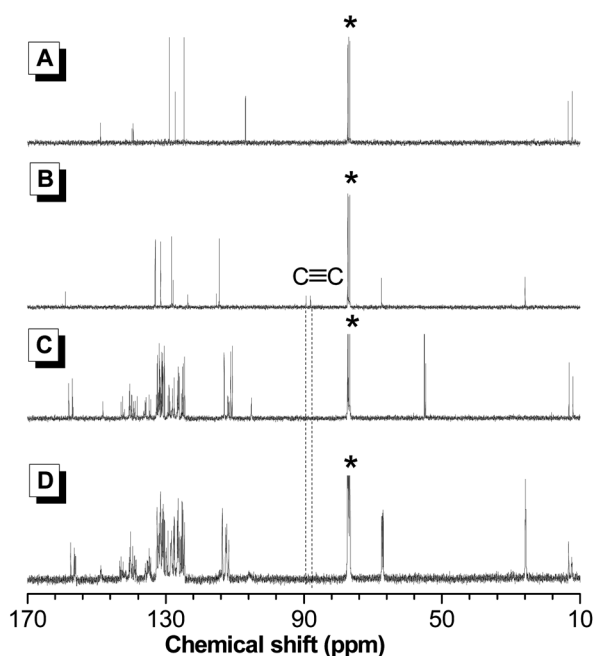spectrum of **P1/2**(4). The methyl proton resonances at δ 2.31 and 2.30 in **1** also shifted to δ 2.01 after the polymerization. Meanwhile, new peaks emerged at the aromatic absorption regions of δ 7.83–7.78 and 6.42–6.28 in **P1/2**(4) due to the formation of new naphthalene rings in the polymer. The spectrum of **P1/2**(4) resembled those of **5–8** but depicted much broader absorption peaks, revealing its polymeric nature.

The ^{13}C NMR spectrum of **P1/2**(4) exhibited no resonance peaks of acetylene carbon atoms of **2**(4) at δ 89.2 and 88.9 (Fig. 2). Its spectral pattern largely resembled those of **5–8**, confirming that the polymeric product was indeed **P1/2**(4) with a molecular structure as shown in Scheme 2. Similar observations were also found in other polymers (Fig. S2–S9†).

Thermal stability

The thermal stability of **P1/2**(m) and **P1/3** was evaluated by thermogravimetric analysis (TGA). As shown in Fig. 3, all the polymers were thermally stable, losing 5% (T_d) of their weight at temperatures higher than 300 °C under nitrogen. Among them, polymer **P1/3** showed the highest thermal stability ($T_d = 422$ °C), which might be ascribed to its higher aromatic content.

Light refraction

Polymers with high refractive indices (RI or n) are promising candidate materials for various practical applications, including lenses, prisms, optical waveguides and holographic image recording systems.[14] As **P1/2**(m) and **P1/3** are constructed from aromatic rings, they may show high refractive indices. Indeed, light yellow transparent thin films of the polymers deposited on a silica substrate showed high RI values (1.747–1.593) in a wide wavelength region of 400–1000 nm (Fig. 4).

The RI values of the polymers at 632.8 nm were all >1.61 (Table 4), which were much higher than those of the commercially important optical plastics, such as polyacrylate ($n =$ 1.492), polycarbonate ($n = 1.581$) and polystyrene ($n = 1.587$). The magnitude of the RI value at 632.8 nm was in the order of **P1/3** (1.725) > **P1/2**(4) (1.628) > **P1/2**(6) (1.625) > **P1/2**(8) (1.617) > **P1/2**(10) (1.613), which was in some sense expected and was in

Fig. 2 ^{13}C NMR spectra of CDCl$_3$ solutions of (A) **1**, (B) **2**(4), (C) a mixture of **5–8** and (D) **P1/2**(4) (sample taken from Table 3, no. 1). The solvent peaks are marked with asterisks.
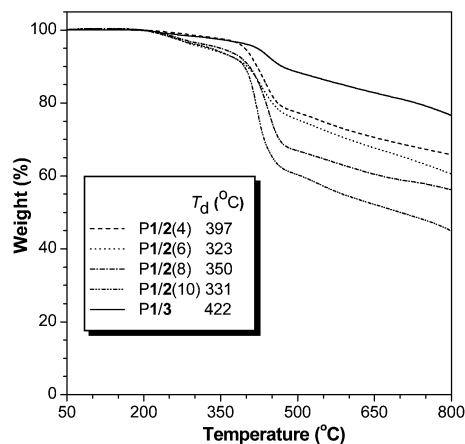

Fig. 3 TGA thermograms of **P1/2**(m) and **P1/3** recorded under nitrogen at a heating rate of 10 °C min^{-1}.
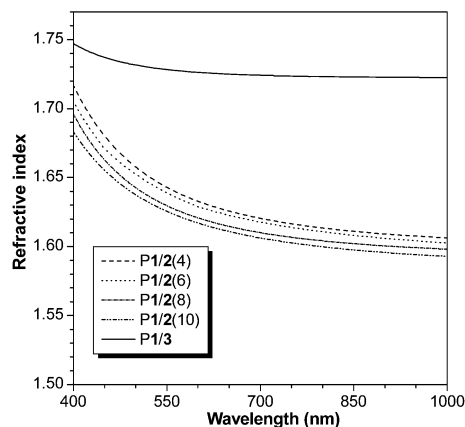
Fig. 4 Wavelength dependence of refractive index of thin films of **P1/2**(m) and **P1/3**.

Table 4 Refractive indices and chromatic dispersions of **P1/2**[a]

No.	Polymer	$n_{632.8}$	ν_D	D
1	**P1/2**(4)	1.6278	16.7239	0.0598
2	**P1/2**(6)	1.6245	18.0229	0.0555
3	**P1/2**(8)	1.6165	18.6389	0.0537
4	**P1/2**(10)	1.6128	19.6315	0.0509
5	**P1/3**	1.7254	91.8275	0.0109

[a] All data were taken from Fig. 4. Abbreviation: n = refractive index (at 632.8 nm). ν_D = Abbé number = $(n_D - 1)/(n_F - n_C)$, where n_D, n_F and n_C are the RI values at wavelengths of Fraunhofer D, F and C spectral lines of 589.2, 486.1 and 656.3 nm, D = chromatic dispersion = $1/\nu_D$.

good correlation with their aromatic content. The Abbé number (ν_D) of a material is a measure of the variation or dispersion in its RI value with wavelength. The ν_D values of **P1/2**(m) and **P1/3** were in the range of ~16–92, corresponding to D values of 0.01–0.06. Thus, the high refractivity and low optical dispersion of the polymers make them promising optical materials.

Optical property

The UV spectrum of a diluted THF solution (10 μM) of **P1/2**(4) exhibited a broad hump centered at ~303 nm (Fig. 5). The spacer length exerts little influence on the ground-state electronic transitions: the UV spectra of **P1/2**(6), **P1/2**(8) and **P1/2**(10) are practically the same as that of **P1/2**(4). On the contrary, **P1/3** absorbs at the redder region with higher intensity, thanks to the conjugated TPE unit. The absorption maximum (327 nm) occurs at a much longer wavelength than that of TPE (299 nm),[12e] indicative of extensive conjugation in the polymer system owing to the electronic communication between the peripheral TPE unit and the central naphthalene core.

Since TPE is an archetypical AIE luminogen, **P1/3** is anticipated to be AIE-active. This is indeed the case, as suggested by the photographs of its THF solution and THF–water mixtures shown in Fig. 6A. While the pure THF solution of **P1/3** emitted no light upon UV irradiation, weak green emission was observed in a THF–H₂O mixture with 20% water content, whose intensity increases on increasing the water content.
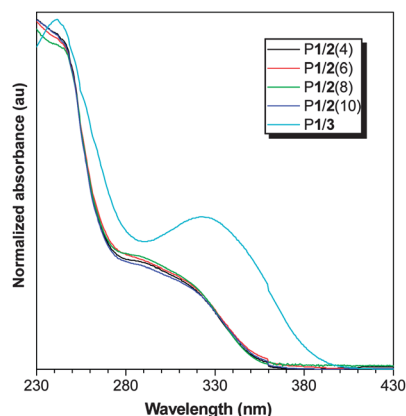

Fig. 5 Normalized UV spectra of **P1/2**(m) and **P1/3** in THF solutions. Concentration: 10 μM.
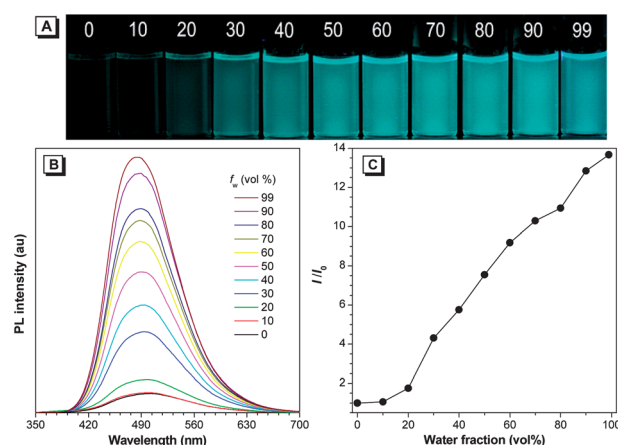

Fig. 6 (A) Photographs of **P1/3** in THF–H₂O mixtures with different water fractions (f_w) taken under 365 nm UV irradiation from a hand-held UV lamp. (B) PL spectra of **P1/3** in THF and THF–water mixtures with different f_w values. Concentration: 10 mM; excitation wavelength: 322 nm. (C) Plot of relative PL intensity (I/I_0) versus the solvent composition of THF–water mixtures of **P1/3**.

Instead of visual observation, we also measured the photoluminescence (PL) of **P1/3** in the solution and aggregated states using a spectrofluorometer. A weak broad peak centered at ~490 nm was recorded in THF solution and THF–water mixtures with low water contents (Fig. 6B). The spectral pattern remained unchanged but the PL intensity rose gradually with an increase in the water content. From THF solution to aqueous mixture with 99% water content, the relative PL intensity increased by ~14-fold (Fig. 6C). Because **P1/3** is insoluble in water, its chains must have been aggregated in aqueous mixtures with high water contents. However, the aqueous mixture is homogeneous without precipitates even at a water content of 99%, revealing that the particles are of nanodimension. To prove this, we analyzed the particle size of **P1/3** in a 99% aqueous mixture using a zeta potential analyzer (Fig. S10†), from which particles with a mean diameter of ~146 nm and a polydispersity of 0.11 were deduced. Evidently, **P1/3** exhibits the AIE phenomenon, whose mechanism is ascribed to the restriction of intramolecular rotation of the

peripheral phenyl rings of the TPE unit in the aggregated state.[11] The fluorescence quantum yield (Φ_F) of **P1/3** in a THF solution calculated using quinine sulfate in 0.1 M sulphuric acid (Φ_F = 54%) was merely 1.91%, which rose to 20.47% in the 99% aqueous mixture (Fig. S11†). Clearly, unlike conventional conjugated polymers, aggregate formation has enhanced, instead of quenching, the light emission of **P1/3**.

Explosive detection

The AIE feature of **P1/3** encourages us to explore its potential application as a fluorescent chemosensor for detecting explosives because of the involved potential anti-terrorism implication.[15] 2,4,6-Trinitrophenol (picric acid, PA) is used as a model compound because it is commercially available, while nano-aggregates of **P1/3** in a 99% aqueous mixture were utilized as the explosive probe. As shown in Fig. 7A, with an increase in the amount of PA in the aqueous mixture, the PL of **P1/3** was weakened progressively. The fluorescence quenching could be clearly observed at a PA concentration as low as 10 μM. At a PA concentration of 0.4 mM, the emission from the polymer was quenched completely. The Lewis acid–base interactions between the electron-rich polymer chains and electron-deficient PA molecules may be responsible for the emission quenching process. The Stern–Volmer plot of relative PL intensity ($I_0/I - 1$) versus the PA concentration gave an upward bending curve instead of a linear line (Fig. 7B), indicative of a super-amplification effect.[16] Large quenching constants up to 289, 500 M^{-1} were deduced from the plot, which were higher than those of polysiloles and polygermoles reported previously (6710–11 000 M^{-1}) in solutions.[17] When a PA molecule enters the three-dimensional network of nanoaggregates of **P1/3** in an aqueous mixture, it may quench the light emission of multiple TPE units in the vicinity. This makes the PL of the nano-aggregates of the polymer highly susceptible to the quencher concentration, thus resulting in the observed superquenching effect.

For real-world applications, it is preferable to perform the detection on a solid support because it requires no complex and expensive equipment and is thus simple, quick and convenient.
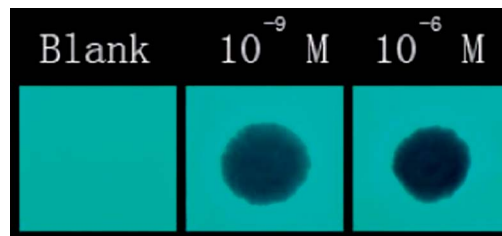
Fig. 8 Fluorescent photographs of **P1/3** coated on TLC plates before and after spotting with aqueous PA solutions with different concentrations.

With such regard, we tested whether the PA sensing can be performed in the solid state. We first coated chains of **P1/3** on TLC plates by dipping the plates into the polymer solution. After solvent evaporation, aqueous PA solutions of different concentrations were spotted on the plates using a capillary tube to give circles with an area of ~0.5 cm^2. When observed under 365 nm UV irradiation from a hand-held UV lamp, the blank plate gave strong blue-green emission, whereas the spotted area showed no light due to the emission quenching by the PA molecules (Fig. 8). The appearance between the bright and dark portions was so different that it enabled lowering the detection limit down to 10^{-9} M.

Conclusions

In this work, we developed a new polymerization route for atom-economical synthesis of functional polymers. Oxidative polycoupling of phenylpyrazole and internal diynes was mediated by [Cp*RhCl$_2$]$_2$, C$_5$H$_2$Ph$_4$ and Cu(OAc)$_2$·H$_2$O under stoichiometric imbalance conditions in DMF for 3 h, generating poly(pyrazolylnaphthalene)s with high molecular weights in satisfactory yields. The polymers were completely soluble, film-forming and thermally stable. Thin solid films of the polymers exhibited high refractive indices (RI = 1.747 − 1.593) in a wide wavelength region of 400–1000 nm. The TPE-containing poly(pyrazolylnaphthalene) was AIE-active and its nanoaggregates worked as sensitive chemosensors for detecting explosives in both solution and solid states.

Experimental section

General information

Tetrahydrofuran (THF) was distilled under nitrogen from sodium benzophenone ketyl immediately prior to use. Dimethylformamide (DMF) was distilled over calcium hydride and stored over molecular sieves. The rhodium complex [RhCp*Cl$_2$]$_2$, named 1,2,3,4-tetramethylcyclopentadienylrhodium(III) chloride dimer, was prepared according to the literature method.[18] Chemicals such as copper(II) acetate monohydrate Cu(OAc)$_2$·H$_2$O, silver 4-toluenesulfonate (AgOTs), silver trifluoromethanesulfonate (AgCF$_3$SO$_3$) and silver trifluoromethanecarboxylate (AgCF$_3$CO$_2$), and other reagents were all purchased from Aldrich and used as received without further purification.

Weight- (M_w) and number-average (M_n) molecular weights and polydispersities (M_w/M_n) of the polymers were estimated by
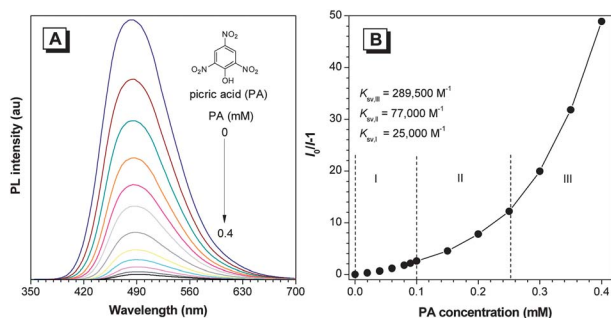

Fig. 7 (A) PL spectra of **P1/3** in THF–water mixtures with 99% water fraction containing different amounts of picric acid (PA). (B) Stern–Volmer plot of ($I_0/I - 1$) values versus PA concentrations in 99% aqueous mixtures of **P1/3**. I_0 = peak intensity at [PA] = 0 M. Concentration: 10 μM; excitation wavelength: 322 nm. Inset: (A) chemical structure of PA.

a Waters Gel Permeation Chromatography (GPC) system equipped with a Waters 515 HPLC pump, a set of Styragel columns (HT3, HT4 and HT6; molecular weight range: 10^2 to 10^7), a column temperature controller, a Waters 486 wavelength-tunable UV-vis detector, a Waters 2414 differential refractometer and a Waters 2475 fluorescence detector. The polymers were dissolved in THF ($\sim$1 mg mL^{-1}) and filtered through 0.45 μm PTFE syringe-type filters before being injected into the GPC system. THF was used as an eluent at a flow rate of 1.0 mL min^{-1}. The column temperature was maintained at 40 °C and the working wavelength of the UV-vis detector was set at 254 nm. A set of monodispersed polystyrene standards (Waters) covering the molecular weight range of 10^3 to 10^7 were used for the molecular weight calibration. IR spectra were recorded on a Perkin-Elmer 16 PC FTIR spectrophotometer. ^{1}H and ^{13}C NMR spectra were measured on Bruker ARX 400 NMR spectrometers using chloroform-d as the solvent. High resolution mass spectra (HRMS) were recorded on a GCT Premier CAB 048 mass spectrometer operated in a MALDI-TOF model. Thermogravimetric analyses (TGA) were conducted under nitrogen on a Perkin-Elmer TGA 7 analyzer at a heating rate of 10 °C min^{-1}. Particle sizes of the polymer aggregates in a THF–water mixture were measured on a BeCoulter Delsa 440SX Zeta potential analyzer. Refractive indices were determined on a J A Woollam Variable Angle Ellipsometry System with a wavelength tunability from 300 to 1000 nm.

Monomer synthesis

Monomer **3** was prepared according to a modified literature method[19] as stated below. To a suspended solution of 1,2-bis-(4-bromophenyl)-1,2-diphenylethene (0.98 g, 2.0 mmol) in triethylamine (30 mL) and toluene (15 mL), triphenylphosphine (105 mg, 0.40 mmol), copper(I) iodide (76 mg, 0.40 mmol) and Pd(PPh$_3$)$_2$Cl$_2$ (140 mg, 0.20 mmol) were added under nitrogen. Phenylacetylene (0.66 mL, 6.0 mmol) was then injected through a septum under stirring and the reaction mixture was heated to 80 °C for 12 h. After being cooled to room temperature, the reaction mixture was dried under vacuum and extracted with CH$_2$Cl$_2$ (60 mL × 3). The organic layers were combined and dried over Na$_2$SO$_4$. After filtration and solvent evaporation, the crude product was purified by silica gel column chromatography using petroleum ether/ethyl acetate as the eluent. Yellow solid; yield 80% (0.85 g). IR (KBr), ν (cm^{-1}): 3027, 1594, 1495, 1440, 753, 694. ^{1}H NMR (CDCl$_3$, 400 MHz), δ (ppm): 7.50–7.47 (m, 4H), 7.32–7.24 (m, 10H), 7.14–6.99 (m, 14H). ^{13}C NMR (CDCl$_3$, 100 MHz), δ (ppm): 143.1, 143.0, 142.51, 142.46, 140.3, 131.0, 130.9, 130.8, 130.7, 130.5, 130.4, 127.7, 127.6, 127.3, 127.2, 126.3, 126.2, 122.7, 120.8, 120.6, 89.2, 89.1, 88.90, 88.86. HRMS (MALDI-TOF): m/z 532.2186 (M$^+$, calcd 532.2191).

Model reaction

In a 15 mL Schlenk tube with a three-way stopcock on the sidearm [RhCp*Cl$_2$]$_2$ (2.47 mg, 0.004 mmol), C$_5$H$_2$Ph$_4$ (5.95 mg, 0.016 mmol), Cu(OAc)$_2$·H$_2$O (40 mg, 0.20 mmol), **1** (34.4 mg, 0.20 mmol) and **4** (41.6 mg, 0.20 mmol) were placed under nitrogen. Freshly dried DMF (0.5 mL) was then injected into the

tube using a hypodermic syringe. The resulting mixture was stirred at 80 °C under nitrogen for 3 h. The reaction mixture was then cooled to room temperature and extracted with CH$_2$Cl$_2$ (30 mL × 3). The organic layer was washed with water (50 mL × 3) and dried over Na$_2$SO$_4$. After purification by silica gel column chromatography using a hexane–ethyl acetate mixture as the eluent, a yellow solid of a mixture of **5–8** (53.3 mg, 91%) was obtained. IR (KBr), ν (cm^{-1}): 1281, 1236, 1171 (C–O stretching). ^{1}H NMR (CDCl$_3$, 400 MHz), δ (ppm): 7.79–5.20 (aromatic protons), 3.75, 3.63, 3.56, 3.54, 3.52 (OCH$_3$ protons), 2.04, 2.02, 2.00 (CH$_3$ protons). ^{13}C NMR (CDCl$_3$, 100 MHz), δ (ppm): 158.0–110.7, 55.1, 55.0, 54.7, 13.2, 12.1. HRMS (MALDI-TOF): m/z 586.2661 (M$^+$, calcd 586.2620).

Polymerization

All the polymerization reactions were carried out under nitrogen atmosphere using a standard Schlenk technique. A typical procedure for the polymerization of **1** and **2**(4) is given below as an example.

In a 15 mL Schlenk tube with a three-way stopcock on the sidearm [RhCp*Cl$_2$]$_2$ (2.47 mg, 0.004 mmol), C$_5$H$_2$Ph$_4$ (5.95 mg, 0.016 mmol), Cu(OAc)$_2$·H$_2$O (40 mg, 0.20 mmol), **1** (34.4 mg, 0.20 mmol) and **2**(4) (44.2 mg, 0.10 mmol) were placed under nitrogen. Freshly distilled DMF (0.5 mL) was then injected into the tube using a hypodermic syringe. The resulting mixture was stirred at 80 °C under nitrogen for 3 h. The solution was added dropwise into 200 mL of methanol *via* a cotton filter under stirring. The precipitate was allowed to stand overnight and then collected by filtration. The polymer was washed with methanol and dried under vacuum at room temperature to a constant weight. A brown powder of polymer **P1/2**(4) was obtained in 82% yield. M_w: 26 300; M_w/M_n: 1.50 (Table 3, no. 1). IR (KBr), ν (cm^{-1}): 1280, 1236, 1170, 1105, 1019 (C–O stretching). ^{1}H NMR (CDCl$_3$, 400 MHz), δ (ppm): 7.83–5.34 (aromatic protons), 3.97–3.67 (OCH$_3$ protons), 2.01–1.66 (CH$_3$ protons). ^{13}C NMR (CDCl$_3$, 100 MHz), δ (ppm): 157.5, 156.5, 156.3, 142.9–111.8, 67.4, 67.3, 67.0, 25.8, 13.3, 12.4.

P1/2(6). Brown powder; yield: 74%. M_w: 27 300; M_w/M_n: 1.53 (Table 3, no. 2). IR (KBr), ν (cm^{-1}): 1281, 1236, 1171, 1106, 1019 (C–O stretching). ^{1}H NMR (CDCl$_3$, 400 MHz), δ (ppm): 7.40–5.43 (aromatic protons), 3.92–3.70 (OCH$_3$ protons), 2.01–1.33 (CH$_3$ protons). ^{13}C NMR (CDCl$_3$, 100 MHz), δ (ppm): 157.6, 156.8, 140.4–111.9, 67.7, 67.6, 67.4, 29.1, 25.8, 13.5, 12.5.

P1/2(8). Brown powder; yield: 79%. M_w: 26 000; M_w/M_n: 1.58 (Table 3, no. 3). IR (KBr), ν (cm^{-1}): 1280, 1237, 1171, 1106, 1023 (C–O stretching). ^{1}H NMR (CDCl$_3$, 400 MHz), δ (ppm): 7.85–5.44 (aromatic protons), 3.92–3.68 (OCH$_3$ protons), 2.08–1.21 (CH$_3$ protons). ^{13}C NMR (CDCl$_3$, 100 MHz), δ (ppm): 157.6, 156.7, 156.5, 140.7–111.7, 67.8, 67.7, 67.5, 29.2, 29.1, 25.8, 13.5, 12.5, 10.3.

P1/2(10). Brown powder; yield: 77%. M_w: 35 700; M_w/M_n: 1.66 (Table 3, no. 4). IR (KBr), ν (cm^{-1}): 1282, 1241, 1174, 1107, 1028 (C–O stretching). ^{1}H NMR (CDCl$_3$, 400 MHz), δ (ppm): 7.84–5.29 (aromatic protons), 3.91–3.68 (OCH$_3$ protons), 2.07–1.21 (CH$_3$ protons). ^{13}C NMR (CDCl$_3$, 100 MHz), δ (ppm): 157.7, 156.7, 149.1–105.6, 67.9, 67.8, 67.6, 29.4, 29.1, 26.0, 25.9, 13.5, 12.3.

P1/3. Brown powder; yield: 66%. M_w: 17 900; M_w/M_n: 1.71 (Table 3, no. 5). IR (KBr), ν (cm^{-1}): 3023, 1599, 1553, 1492, 1439, 1382, 751, 696 (C–O stretching). ^{1}H NMR (CDCl$_3$, 400 MHz), δ (ppm): 7.82–6.42 (aromatic protons), 2.05–1.99 (CH$_3$ protons). ^{13}C NMR (CDCl$_3$, 100 MHz), δ (ppm): 149.3–105.8, 13.5, 12.3.

Acknowledgements

References

1 (a) H. Shirakawa, *Angew. Chem., Int. Ed.*, 2001, **40**, 2574–2580; (b) A. G. MacDiarmid, *Angew. Chem., Int. Ed.*, 2001, **40**, 2581–2590; (c) A. J. Heeger, *Angew. Chem., Int. Ed.*, 2001, **40**, 2591–2611.

2 (a) J. L. Liu, J. W. Y. Lam and B. Z. Tang, *Chem. Rev.*, 2009, **109**, 5799–5867; (b) A. Qin, J. W. Y. Lam and B. Z. Tang, *Chem. Soc. Rev.*, 2010, **39**, 2522–2544; (c) J. W. Y. Lam and B. Z. Tang, *Acc. Chem. Res.*, 2005, **38**, 745–754; (d) A. Qin, J. W. Y. Lam and B. Z. Tang, *Prog. Polym. Sci.*, 2012, **37**, 182–209; (e) S. K. Choi, Y. S. Gal, S. H. Jin and H. K. Kim, *Chem. Rev.*, 2000, **100**, 1645–1681; (f) H. F. Bunz, *Acc. Chem. Res.*, 2001, **34**, 998–1010; (g) M. B. Nielsen and F. Diederich, *Chem. Rev.*, 2005, **105**, 1837–1867; (h) W. Zhang and J. S. Moore, *Angew. Chem., Int. Ed.*, 2006, **45**, 4416–4439; (i) T. J. Masuda, *J. Polym. Sci., Part A: Polym. Chem.*, 2007, **45**, 165–180; (j) J. Wu, W. Pisula and K. Mullen, *Chem. Rev.*, 2007, **107**, 718–747; (k) S. W. Thomas, G. D. Joly and T. Swager, *Chem. Rev.*, 2007, **107**, 1339–1386; (l) Y. Morisakia and Y. Chujo, *Prog. Polym. Sci.*, 2008, **33**, 346–364.

3 For selected examples of polycyclotrimerization, see: (a) J. B. Shi, C. J. W. Jim, F. Mahtab, J. Z. Liu, J. W. Y. Lam, H. H. Y. Sung, I. D. Williams, Y. P. Dong and B. Z. Tang, *Macromolecules*, 2010, **43**, 680–690; (b) J. Z. Liu, L. Zhang, J. W. Y. Lam, C. K. W. Jim, Y. A. Yue, R. Deng, Y. N. Hong, A. J. Qin, H. H. Y. Sung, I. D. Williams, G. C. Jia and B. Z. Tang, *Macromolecules*, 2009, **42**, 7367–7378; (c) H. Li, J. Wang, J. Z. Sun, R. Hu, A. Qin and B. Z. Tang, *Polym. Chem.*, 2012, **3**, 1075–1083, For selected examples of Diels–Alder reactions, see: (d) H. Mukamal, F. W. Harris and J. K. Stille, *J. Polym. Sci., Part A: Polym. Chem.*, 1967, **5**, 2721–2729; (e) A. L. Rusanov, D. Y. Likhachev, P. V. Kostoglodov and N. M. Belomoina, *Polym. Sci., Ser. C*, 2008, **50**, 39–62.

4 M. Saleh, M. Baumgarten, A. Mavrinskiy, T. Schäfer and K. Müllen, *Macromolecules*, 2010, **43**, 137–143.

5 C. Li, M. Liu, N. G. Pschirer, M. Baumgarten and K. Mullen, *Chem. Rev.*, 2010, **110**, 6817–6855.

6 S. J. Toal and W. C. Trogler, *J. Mater. Chem.*, 2006, **16**, 2871–2883.

7 (a) A. M. Fraind and J. D. Tovar, *J. Phys. Chem. B*, 2010, **114**, 3104–3116; (b) J. Feng, X. Chen, Q. Han, H. Wang, P. Lu and Y. Wang, *J. Lumin.*, 2011, **131**, 2775–2783; (c) V. C. Sundar, J. Zaumseil, V. Podzoror, E. Menard, R. L. Willett, T. Someya, M. E. Gershenson and J. A. Rogers, *Science*, 2004, **303**, 1644–1646; (d) M. S. Goncalves, *Chem. Rev.*, 2009, **109**, 190–212; (e) S. Li, J. Xiang, X. Mei and C. Xu, *Tetrahedron Lett.*, 2008, **49**, 1690–1693.

8 For selected examples of polymerizations under stoichiometric imbalance conditions: (a) K. Wakabayashi, S. I. Kohama, S. Yamazaki and K. Kimura, *Macromolecules*, 2008, **41**, 1168–1174; (b) D. Zhao and K. Yue, *Macromolecules*, 2008, **41**, 4029–4036; (c) N. Nomura, K. Tsurugi and M. Okada, *Angew. Chem., Int. Ed.*, 2001, **40**, 1932–1935; (d) N. Nomura, K. Tsurugi, T. V. RajanBabu and T. Kondo, *J. Am. Chem. Soc.*, 2004, **126**, 5354–5355; (e) T. Takemura, K. Sugie, H. Nishino, S. Kawabata and T. Koizumi, *J. Polym. Sci., Part A: Polym. Chem.*, 2008, **46**, 2250–2261; (f) N. Kihara, S. Komatsu, T. Takata and T. Endo, *Macromolecules*, 1999, **32**, 4776–4783; (g) H. Iimori, Y. Shibasaki, S. Ando and M. Ueda, *Macromol. Symp.*, 2003, **199**, 23–35; (h) T. Dutta, K. B. Woody and M. D. Watson, *J. Am. Chem. Soc.*, 2008, **130**, 452–453; (i) A. R. Cruz, M. C. G. Hernandez, M. T. Guzmán–Gutiérrez, M. G. Zolotukhin, S. Fomine, S. L. Morales, H. Kricheldorf, E. S. Wilks, J. Cárdenas and M. Salmón, *Macromolecules*, 2012, **45**, 6774–6780; (j) H. R. Kricheldorf, M. G. Zolotukhin and J. Cardenas, *Macromol. Rapid Commun.*, 2012, **33**, 1814–1832.

9 M. Gao, J. W. Y. Lam, J. Li, C. Y. K. Chan, Y. Chen, N. Zhao, T. Han and B. Z. Tang, *Polym. Chem.*, 2013, **4**, 1372–1380.

10 (a) N. Umeda, K. Hirano, T. Satoh, N. Shibata, H. Sato and M. Miura, *J. Org. Chem.*, 2011, **76**, 13–24; (b) N. Umeda, H. Tsurugi, T. Satoh and M. Miura, *Angew. Chem., Int. Ed.*, 2008, **47**, 4019–4022.

11 Z.-X. Wang and H.-L. Qin, *Green Chem.*, 2004, **6**, 90–92.

12 (a) Y. Hong, J. W. Lam and B. Z. Tang, *Chem. Soc. Rev.*, 2011, **40**, 5361–5388; (b) Y. Hong, J. W. Y. Lam and B. Z. Tang, *Chem. Commun.*, 2009, 4332–4353; (c) R. Hu, J. W. Y. Lam, J. Liu, H. H. Y. Sung, I. D. Williams, Z. Yue, K. S. Wong, M. M. F. Yuen and B. Z. Tang, *Polym. Chem.*, 2012, **3**, 1481–1489; (d) H. Li, J. Wang, J. Z. Sun, R. Hu, A. Qin and B. Z. Tang, *Polym. Chem.*, 2012, **3**, 1075–1083; (e) Z. Zhao, S. Chen, J. W. Y. Lam, C. K. W. Jim, C. Y. K. Chan, Z. Wang, P. Li, C. Peng, H. S. Kwok, Y. Ma and B. Z. Tang, *J. Phys. Chem. C*, 2010, **114**, 7963–7972.

13 Y. Liu, C. M. Deng, L. Tang, A. J. Qin, R. R. Hu, J. Z. Sun and B. Z. Tang, *J. Am. Chem. Soc.*, 2011, **133**, 660–663.

14 J.-g. Liu and M. Ueda, *J. Mater. Chem.*, 2009, **19**, 8907–8919.

15 (a) S. W. Thomas, G. D. Joly and T. M. Swager, *Chem. Rev.*, 2007, **107**, 1339–1386; (b) D. Zhao and T. M. Swager, *Macromolecules*, 2005, **38**, 9377–9384.

16 (a) J. Liu, Y. Zhong, P. Lu, Y. Hong, J. W. Y. Lam, M. Faisal, Y. Yu, K. S. Wong and B. Z. Tang, *Polym. Chem.*, 2010, **1**, 426–429.

17 H. Sohn, M. J. Sailor, D. Magde and W. C. Trogler, *J. Am. Chem. Soc.*, 2003, **125**, 3821–3830.

18 J. W. Kang, K. Moseley and P. M. Maitlis, *J. Am. Chem. Soc.*, 1969, **91**, 5970–5977.

19 V. S. Vyas and R. Rathore, *Chem. Commun.*, 2010, **46**, 1065–1067.